Activator Protein-1 Transcription Factors Are Associated with Progression and Recurrence of Prostate Cancer

Xuesong Ouyang,[1,2] Walter J. Jessen,[6] Hikmat Al-Ahmadie,[7] Angel M. Serio,[8,10] Yong Lin,[4,5] Weichung-Joseph Shih,[4,5] Victor E. Reuter,[7] Peter T. Scardino,[8] Michael M. Shen,[1,3,5] Bruce J. Aronow,[6] Andrew J. Vickers,[8,10] William L. Gerald,[7,9] and Cory Abate-Shen[1,2,5]

[1]Center for Advanced Biotechnology and Medicine, Departments of [2]Medicine, [3]Pediatrics, and [4]Biometrics, [5]The Cancer Institute of New Jersey, University of Medicine and Dentistry, New Jersey-Robert Wood Johnson Medical School, Piscataway, New Jersey; [6]Department of Biomedical Informatics, Cincinnati Children's Hospital Medical Center, University of Cincinnati College of Medicine, Cincinnati, Ohio; Departments of [7]Pathology, [8]Surgery (Urology), [9]Human Oncology and Pathogenesis, and [10]Epidemiology and Biostatistics, Memorial Sloan Kettering Cancer Center, New York, New York

Abstract

To identify biomarkers that discriminate the aggressive forms of prostate cancer, we performed gene expression profiling of prostate tumors using a genetically engineered mouse model that recapitulates the stages of human prostate cancer, namely *Nkx3.1; Pten* mutant mice. We observed a significant deregulation of the epidermal growth factor and mitogen-activated protein kinase (MAPK) signaling pathways, as well as their major downstream effectors—the activator protein-1 transcription factors *c-Fos* and *c-Jun*. Forced expression of c-Fos and c-Jun in prostate cancer cells promotes tumorigenicity and results in activation of extracellular signal-regulated kinase (Erk) MAPK signaling. In human prostate cancer, up-regulation of c-Fos and c-Jun proteins occurs in advanced disease and is correlated with Erk MAPK pathway activation, whereas high levels of c-Jun expression are associated with disease recurrence. Our analyses reveal a hitherto unappreciated role for AP-1 transcription factors in prostate cancer progression and identify c-Jun as a marker of high-risk prostate cancer. This study provides a striking example of how accurate mouse models can provide insights on molecular processes involved in progression and recurrence of human cancer. [Cancer Res 2008;68(7):2132–44]

Introduction

Recent advances in detection and treatment of organ-confined prostate cancer have significantly improved the prognosis for men with the disease. However, prostate tumors vary in their degree of aggressiveness: Whereas many are fairly indolent and readily curable by surgery or radiation therapy, some are more aggressive and have less favorable outcomes. Current modalities for distinguishing indolent from aggressive forms of the disease are largely reliant on the clinical behavior and/or morphologic features of the tumors, such as Gleason grade and tumor-node-metastases score, rather than molecular properties. Indeed, the identification of relevant biomarkers has been hampered by characteristic features of prostate cancer, including its multifocality and heterogeneity (1), limitations involving tissue procurement and related issues (2), and broader challenges facing the application of genomic analyses for improving the diagnosis and treatment of cancer patients (3).

These limitations can be overcome, in part, through analyses of genetically engineered mouse models, which can lead to the identification of molecular pathways of human cancer progression as well as biomarkers for stratification of cancer patients (4–6). In our studies, we have used a mouse model of prostate cancer based on the combined inactivation of the *Nkx3.1* homeobox gene and the *Pten* tumor suppressor, which are relevant for human prostate cancer (7–9). *NKX3.1* is located in a region of human chromosome 8p21, which is frequently lost at early stages of prostate tumorigenesis (reviewed in ref. 9). *PTEN* is deregulated in many cancers, including prostate, where its function is critically associated with androgen receptor signaling (reviewed in refs. 7, 10). Mice that are compound heterozygotes for null alleles of *Nkx3.1* and *Pten* (herein referred to as *Nkx3.1; Pten* mutant mice) recapitulate the stages of human prostate cancer progression and display many salient features of prostate tumorigenesis (11–13).

In the present study, we have used *Nkx3.1; Pten* mutant mice to investigate molecular pathways that are deregulated during prostate cancer progression. Our results highlight a central role for the AP-1 transcription factors, c-Fos and c-Jun (herein referred to as Fos and Jun), which can function as heterodimeric complexes, as well as a homodimer in the case of Jun, to regulate gene expression (14). Most notably, our analyses of the *Nkx3.1; Pten* mutant mice has led to discovery that Jun is associated with disease recurrence in human prostate cancer. These findings show how analyses of accurate mouse models can provide insights regarding molecular pathways of progression and recurrence of human cancer.

Materials and Methods

Gene expression profiling and data analyses. Generation and analysis of mutant mice harboring germ-line null alleles of *Nkx3.1* and/or *Pten* have been described (13, 15, 16). For gene expression profiling, we used strain- and age-matched wild-type and mutant mice representing dysplasia, low-grade and high-grade prostatic intraepithelial neoplasia (PIN), adenocarcinoma, and androgen-independent disease (four or more independent cases per stage), which are described in Supplementary Table S1. Following

Note: Supplementary data for this article are available at Cancer Research Online (http://cancerres.aacrjournals.org/).

Present address for C. Abate-Shen: Department of Urology, Columbia University, College of Physicians and Surgeons, Herbert Irving Cancer Center, New York, NY 10032. Present address for H. Al-Ahmadie: Department of Pathology, University of Chicago Medical Center, Chicago, IL 60637.

Requests for reprints: Cory Abate-Shen, Department of Urology, Columbia University, College of Physicians and Surgeons, Herbert Irving Comprehensive Cancer Center, 1130 St. Nicholas Avenue, Room 217A, New York, NY 10032. Phone: 212-851-4731; Fax: 212-851-4572; E-mail: cabateshen@columbia.edu.

doi:10.1158/0008-5472.CAN-07-6055

sacrifice, the individual prostatic lobes (anterior, dorsal, lateral, and ventral) were bilaterally dissected; one side was fixed in formalin for histologic analyses and the other was snap frozen in optimum cutting temperature (Sakura Finetek) for gene expression profiling. Laser capture microdissection (Arcturus Pixcell IIE) was performed to isolate prostate epithelial cells from cryosections of the dorsolateral prostate. RNA was prepared using the PicoPure RNA isolation kit (Arcturus), followed by RNA linear amplification and labeling using Small Sample Labeling Protocol VII (Affymetrix). Biotin-labeled RNA samples were hybridized to Affymetrix GeneChips (MOE430A). GeneChips were scanned for data acquisition using a GeneChip Scanner 3000 (Affymetrix).

Affymetrix Microarray Suite 5.0 was used to generate "CEL" files that were then processed using Robust Multichip Analysis in Bioconductor/R. The gene expression level for each transcript in each sample was set to its ratio relative to the median expression of the transcript across the normal (wild-type) samples. ANOVA ($P \leq 0.1$) was used to compare the following sample groups: normal, dysplasia/low-grade PIN, high-grade PIN/cancer, androgen-independent high-grade PIN, and androgen-independent cancer. Statistical comparisons were performed using GeneSpring GX v7.3.1 (Agilent Technologies). Results from the primary analysis were corrected for multiple testing effects by applying the Benjamini and Hochberg false discovery rate correction (FDR $\leq$0.1). Statistically overrepresented gene ontologies and both KEGG and BioCarta pathways ($P < 0.05$) were identified using the Database for Annotation, Visualization and Integrated Discovery 2007 at the National Institute of Allergy and Infectious Diseases, NIH (17). Construction of the signaling pathway and identification of literature-based gene associations were completed using Ingenuity Pathways Analysis, version 5 (Ingenuity Systems).[11] The genes or gene products are represented as nodes, and the biological relationship between two nodes is represented as an edge (solid line, direct association; dashed line, indirect association). All edges are supported by at least one reference from the literature, a textbook, or canonical information stored in the Ingenuity Pathways Knowledge Base.

Expression validation. For real-time reverse transcription-PCR (RT-PCR), RNA was extracted using Trizol (Invitrogen) and purified using an RNAeasy kit (Qiagen). Following reverse transcription, quantitative PCR was performed using the Mx4000 Multiplex Quantitative PCR system (Stratagene). For Western blot analyses, protein extracts from prostate tissues or cultured cells were made by sonication in buffer containing 10 mmol/L Tris-HCl (pH 7.5), 0.15 mol/L NaCl, 1 mmol/L EDTA, 0.1% SDS, 1% deoxycholate (sodium salt), and 1% Triton X-100 with freshly added protease inhibitor and phosphatase inhibitor cocktail (Sigma). Immunohistochemical analyses were performed on formalin-fixed, paraffin-embedded tissues as described (12, 13). Antibodies were as follows: Clusterin (Santa Cruz Biotechnology, 1:250), Hepsin (Cayman, 1:500), c-Jun (Cell Signaling, 1:100 for immunohistochemistry and 1:500 for Western blots), c-Fos (K-25, Santa Cruz Biotechnology, 1:400 for immunohistochemistry and 1:1,000 for Western blots), and anti–β-tubulin (Sigma, 1:1,000). The Ezh2 antibody was a gift from Dr. Danny Reinberg (Department of Biochemistry, New York University, School of Medicine, New York, NY) (1:2,000).

Functional validation. Functional analyses of Fos and Jun were done using CASP 2.1 cells, an androgen-responsive prostate cell line derived from primary tumors from the *Nkx3.1; Pten* mutant mice (12). Retroviral gene transfer was performed to introduce *Fos* and/or *Jun* into the cells; infection efficacy was >80%. Proliferation assays and anchorage-independent tumor growth assays were performed as described (12, 16) using medium containing charcoal/dextran–treated fetal bovine serum with or without dihydrotestosterone.

For orthotopic tumor assays, 5×10^5 of CASP 2.1 cells expressing Jun and/or Fos (or a control vector) were injected unilaterally into the left dorsal prostate of athymic *nude* male mice. Following 8-wk growth, the dorsal prostates were bilaterally dissected and wet tumor weights were determined by comparing the injected and noninjected sides as described (12). Histologic and immunohistochemical analyses of the tumors were done as described (12).

[11] http://www.ingenuity.com

Prostate tissue microarrays and statistical methods. Tissue microarrays (TMA) were constructed using tissue samples from patients undergoing radical prostatectomy for localized prostate cancer at Memorial Sloan-Kettering Cancer Center between 1985 and 2003. Patients without adequate pathologic material for sampling were excluded. All studies were approved by the institutional review board of Memorial Sloan-Kettering Cancer Center. TMAs were created using an automated tissue arrayer (ATA27, Beecher Instruments). Three representative tissue cores, 0.6 mm in diameter, were extracted from regions of interest for each patient and mounted in paraffin blocks.

Grading of the progression TMA was done in triplicate blindly by two individuals (X.O. and C.A-S.) based on intensity and percentage of positive cells. An average score for immunoreactivity of Jun and Fos was given ranging from 0 to 4 to represent negative ($0 \leq$ score < 1), weak ($1 \leq$ score < 2), moderate ($2 \leq$ score < 3), or robust ($3 \leq$ score < 4) expression. Logistic regression was used to compare the expression of Jun and Fos (defined as a score of 1 or higher) with prostate tumor progression; Spearman correlation coefficient was done to evaluate the association of Jun and/or Fos and/or phosphorylated extracellular signal-regulated kinase (p-Erk) expression.

For grading the outcomes TMA, the immunostained slides were scanned using a whole slide scanner (Scanning Microscope Chromavision ACIS II, DAKO). Each prostate specimen was scored in triplicate blindly and independently by two individuals (X.O. and H.A-A.), and each core was scored based on staining intensity (0–3) and percentage of positive cells (0–100%). This resulted in a maximum of six scores for each patient. For statistical analysis, a single value for each patient was calculated by taking the average of the six scores; those patients with fewer than two scores were not reported. Among 948 patient samples scored, 45 had $\leq$1 score for both Fos and Jun, and an additional 61 patients had incomplete pathologic data. The final cohort therefore comprised 842 patients, 824 of whom had >1 score for Fos and 837 of whom had >1 score for Jun.

Exploratory histograms revealed no obvious dichotomous separation for percentage of positive tumor cells (Supplementary Data); we therefore considered the expression of Fos and Jun as continuous in all statistical analyses. Logistic regression was used to evaluate the association between Fos and Jun expression and pathologic stage (presence or absence of extracapsular extension, seminal vesicle invasion, and lymph node involvement); ordinal logistic regression was used for pathologic grade (Gleason grade); Cox proportional hazards regression was used to test the association between Fos and Jun and two separate time-to-event end points; biochemical recurrence was defined as prostate-specific antigen (PSA) >0.2 ng/mL with a confirmatory level; and clinical failure was defined as radiographic or biopsy evidence of metastases, death from disease, or an increasing PSA in a castrated state (higher than postcastration nadir, confirmed by a subsequent rise $\geq$3 wk later). Predictive accuracy was assessed by the concordance index (*c*-index), which ranges from 0.5 to 1.0. The *c*-index is comparable with the area under the receiver operating characteristic curve and can be used to quantify discrimination of a single variable or a multivariable model for survival-time data (18). All reported *c*-indices are bootstrap corrected with 200 replications. Statistical analyses were conducted using Stata 9.0 (StataCorp.).

Results and Discussion

Conservation of gene expression changes during prostate cancer progression in *Nkx3.1; Pten* mice and humans. Single and compound *Nkx3.1* and *Pten* mutant mice recapitulate stages of human prostate cancer progression in an age- and androgen-dependent manner (11–13, 16). In particular, *Nkx3.1* homozygous mutants ($Nkx3.1^{-/-}$) develop dysplasia by 6 months of age (15, 16), whereas *Nkx3.1; Pten* compound mutants ($Nkx3.1^{+/-}$; $Pten^{+/-}$) develop low-grade PIN by 6 months, high-grade PIN by 9 months, invasive adenocarcinoma with metastatic potential by 12 months, and androgen-independent tumors following androgen ablation (11–13). To identify molecular changes associated with prostate tumorigenesis, we performed gene expression profiling

using wild-type, single, and compound mutant mice representing different stages of prostate cancer (Supplementary Table S1). Analyses were done on Affymetrix microarrays using RNA obtained following laser-capture microdissection of prostate epithelial cells. We focused on the dorsolateral lobe of the mouse prostate, as it is generally considered to be most analogous to the peripheral zone of the human prostate.

Using parametric statistical analysis (ANOVA, FDR ≤0.1), 3,225 genes were identified as differentially expressed among the phenotypic groups (Supplementary Data).[12] These include many that have been previously implicated in prostate or other human cancers, suggesting conservation between the molecular pathways of cancer progression in these mutant mice and human prostate cancer. Indeed, among 22 widely accepted markers of human prostate cancer, we found that more than half (12 of 22) were significantly deregulated ($P < 0.001$) during cancer progression in the *Nkx3.1; Pten* mutant mice, as had been shown previously in human prostate cancer (Fig. 1; Supplementary Table S2). These include the androgen receptor, whose up-regulated expression is of principal relevance for hormone refractory prostate cancer (19); *Clusterin*, an antiapoptotic gene that has been associated with poor prognosis (20); *Ezh2*, a histone methyltransferase that is overexpressed during cancer progression and in hormone-refractory, metastatic prostate cancer (21); and *Hepsin*, a cell surface serine protease that has been associated with metastasis (22). Therefore, the molecular features of prostate cancer progression in the *Nkx3.1; Pten* mice are highly similar to those that are biologically relevant for human prostate cancer.

Fos and Jun are downstream effectors for epidermal growth factor and MAPK signaling pathways during cancer progression. To distinguish causal from coincidental gene expression changes in our expression profiling analysis, we used a functional enrichment approach (17) to identify signaling pathways that are significantly deregulated during cancer progression in the mutant mice, and then focused on key downstream effectors of these pathways. We queried the 3,225 gene list for functional enrichment of gene ontologies and/or signaling pathways and focused on three statistically overrepresented biological themes, namely (*a*) the epidermal growth factor (EGF) signaling pathway; (*b*) regulation of MAPK activity; (*c*) small GTPase–mediated signal transduction (Fig. 2*A*; Table 1). Importantly, each of these pathways and/or gene signatures has been shown to be functionally relevant for progression of human prostate cancer (23).

Among these deregulated genes were the *c-Fos* and *c-Jun* proto-oncogenes, which represent common downstream targets for these signaling pathways (Fig. 2*A*; Table 1). In particular, *c-Fos* and *c-Jun* encode components of the AP-1 transcription factor complex, which is a principal effector of EGF and MAPK signaling, as well as oxidative damage and other stress stimuli (14, 24, 25). In addition, several AP-1 targets, such as matrix metalloproteinases (i.e., *MMP9*), apoptotic regulators (i.e., *BCL2-like 11* and *Bcl-3*), and proliferative regulators (i.e., *Cdkn2a*; refs. 24, 26, 27), were also deregulated in the mutant mice (Supplementary Data), consistent with transcriptional activation of Fos and Jun during cancer progression.

Notably, previous studies have reported that Fos and Jun proteins are up-regulated in human prostate cancer, particularly in hormone-refractory disease (28, 29), where they can modulate the transcriptional activity of the androgen receptor (30–32). However, some studies have found that the levels of *Fos* and/or *Jun* RNA may be reduced in human prostate tumors (e.g., ref. 33), potentially due to surgical manipulation of the tissues (2). This highlights another potential benefit of using mutant mouse models for gene discovery, namely that acquisition of RNA can be optimized for gene expression profiling.

Fos and Jun promote prostate tumorigenicity and activation of Erk MAPK signaling in *Nkx3.1; Pten* mice. To investigate the expression and functions of Fos and Jun in prostate cancer and their relationship to EGF-MAPK signaling in *Nkx3.1; Pten* mice and human prostate cancer, we first confirmed that they were up-regulated during cancer progression in the *Nkx3.1; Pten* mutant mice. Real-time RT-PCR analyses revealed that *Jun* and *Fos* mRNA are expressed at low levels in normal prostate and low-grade PIN, but significantly elevated in androgen-dependent high-grade PIN/cancer (2.8-fold or 3.9-fold, respectively; $P < 0.001$; $n = 6$/group), and further increased in more advanced androgen-independent high-grade PIN/cancer (4.8-fold and 8.3-fold, respectively; $P < 0.0001$; $n = 6$/group; Fig. 2*B*). Expression of Jun and Fos proteins displayed a similar trend in established prostate cancer cell lines from mice and humans, where they were expressed at lower levels in more differentiated, androgen-responsive lines (i.e., CASP 2.1 and LNCaP) and at higher levels in the more highly transformed, androgen-independent cells (i.e., CASP 1.0 and PC3; Fig. 2*C*). Immunohistochemical analyses further confirmed the up-regulated expression of Jun and Fos in *Nkx3.1; Pten* mice with advanced disease, and showed their nuclear localization in prostate epithelial cells ($n = 6$/group; Fig. 2*D*). Interestingly, this pattern of elevated Fos and Jun expression parallels that of Erk MAPK activation that we have previously reported (ref. 12 and below). Overall, although the trends of Fos and Jun expression patterns were similar, the relative levels of Fos were consistently higher than Jun at both the mRNA and protein levels.

To investigate their consequences for prostate tumorigenicity, we introduced Fos and Jun individually or together into CASP 2.1 cells (Fig. 3*A*), an androgen-responsive prostate cancer line (12) that normally expresses low levels of these proteins (see Fig. 2*B*). Although forced expression of either Fos or Jun alone in the CASP 2.1 cells had little effect on growth (data not shown), their coexpression resulted in a significant increase in cellular proliferation (~2-fold, $P < 0.0001$), particularly in the absence of androgens (dihydrotestosterone; Fig. 3*B*). Similarly, coexpression of Fos and Jun displayed a significant increase in anchorage-independent growth, which was most pronounced in the absence of androgens (~7-fold, $P < 0.0001$; Fig. 3*C*). These results show that Fos and Jun promote proliferation and tumorigenicity in culture, particularly in conditions of limiting androgens.

To investigate the effects of Fos and Jun misexpression for prostate tumor growth *in vivo*, we orthotopically implanted CASP 2.1 cells expressing Jun and/or Fos directly into the dorsal prostate of *nude* male mice and monitored tumor size following 8 weeks of growth (Fig. 3*D*). Cells expressing both Fos and Jun formed tumors that were significantly larger (~8 mg) than those formed by control cells or by cells expressing either Fos or Jun alone ($P < 0.0001$; $n = 10$/group; Fig. 3*D*). Similar results were obtained following orthotopic injection of human LNCaP cells expressing Fos and Jun into the dorsal prostate of *nude* male mice (data not shown). The tumors derived from the Fos and Jun coexpressing cells were less differentiated and more highly proliferative relative to tumors from the control cells or from cells expressing Fos or Jun

[12] W.J. Jessen et al., in preparation.

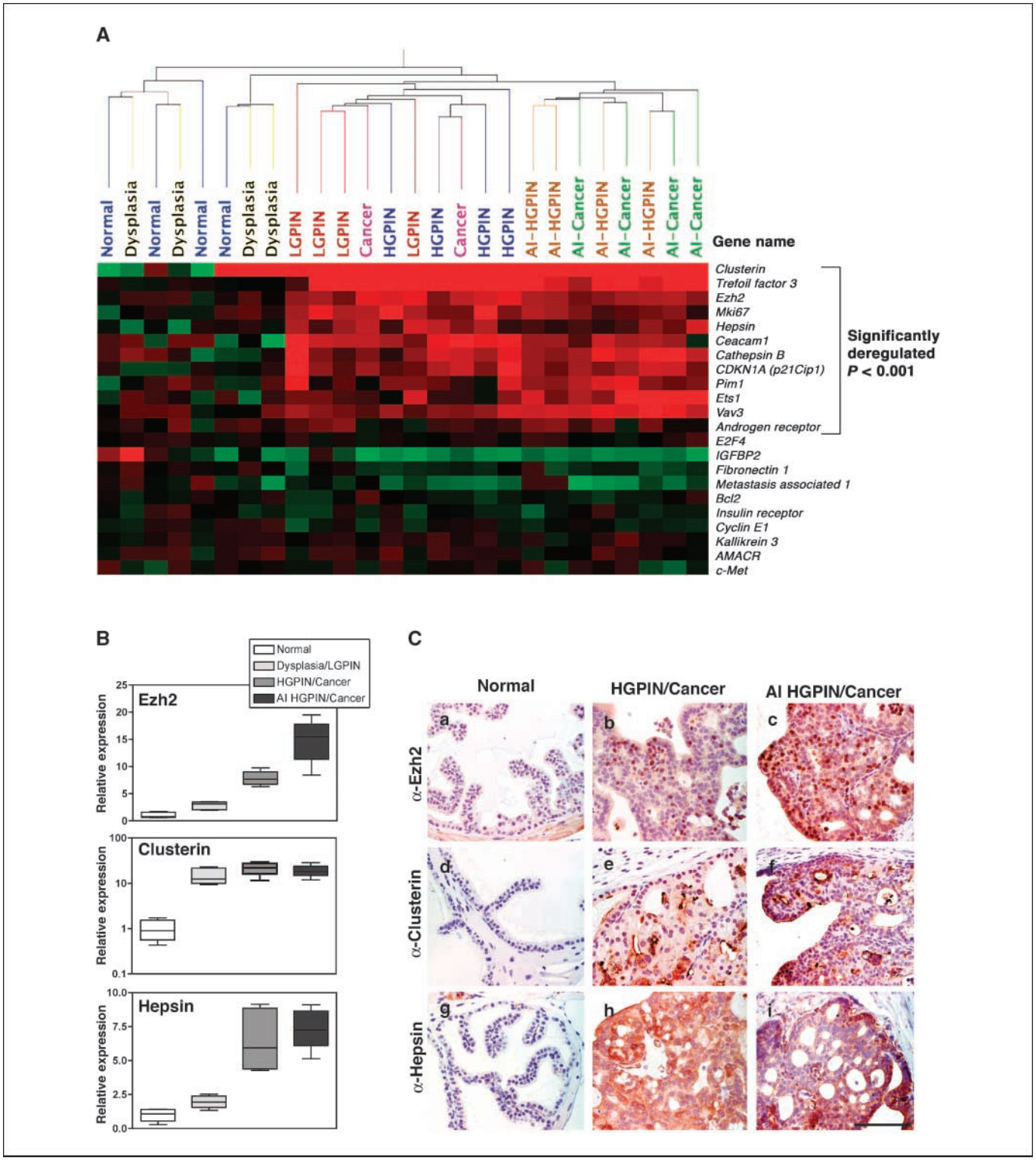

Figure 1. Conservation of gene expression changes during cancer progression in the *Nkx3.1; Pten* mutant mice and human prostate cancer. *A,* expression profiling was done using RNA obtained by laser capture microdissection of dorsal prostate from *Nkx3.1; Pten* wild-type or mutant mice representing normal, dysplasia, low-grade PIN (*LGPIN*), high-grade PIN (*HGPIN*), cancer, or androgen independent high-grade PIN or cancer (*AI-HGPIN* or *AI-Cancer*) as indicated. Hierarchical clustering of the mouse orthologues of genes that are known biomarkers of human cancer progression (Supplementary Table S2). The genes that are significantly deregulated ($P < 0.01$) are indicated. *B,* real-time PCR analysis was performed to evaluate the expression levels of the indicated genes using total RNA from normal prostate, dysplasia/low-grade PIN, high-grade PIN/cancer, or androgen-independent high-grade PIN/cancer (six independent samples per group). Expression levels of the experimental gene were standardized relative to *GADPH* (internal control) and plotted using Prism box and whiskers graph. Note that each of the significant genes shown in *A* and Supplementary Table S2 were validated by real-time PCR; selected data are shown. *C,* immunohistochemical analyses using the indicated antibodies was performed on sections from the anterior prostate of 12-mo wild-type mice (*Nkx3.1*$^{+/+}$*; Pten*$^{+/+}$; normal), or from *Nkx3.1*$^{+/-}$*; Pten*$^{+/-}$ mutant mice that displayed high-grade PIN and cancer (*HGPIN/Cancer*) or androgen-independent high-grade PIN (*AI HGPIN/Cancer*). Representative images (*a–i*) are shown from a minimum of eight independent tissues analyzed in each group. *Bars,* 100 μm.

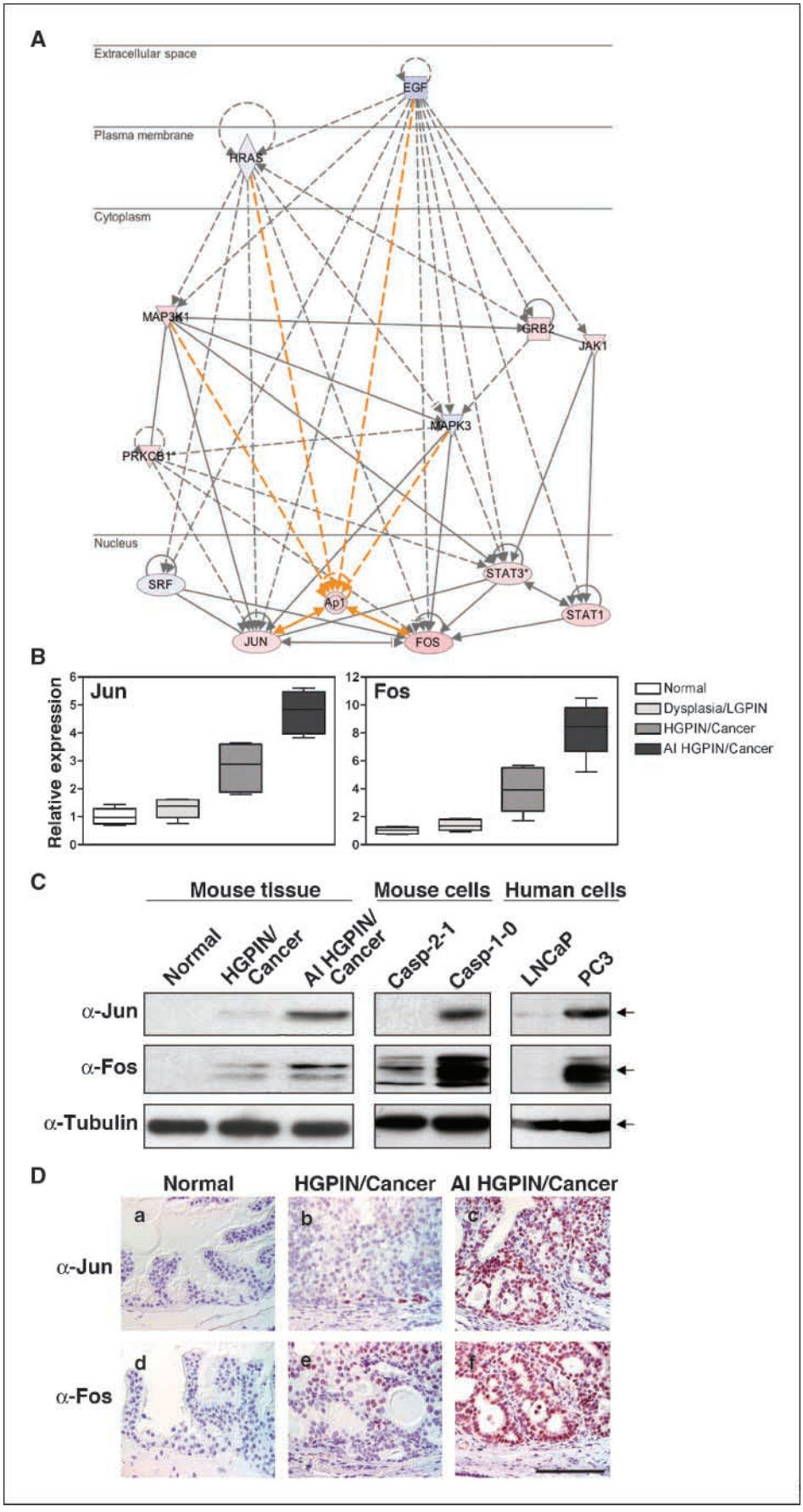

Figure 2. Fos and Jun are downstream effectors for EGF and MAPK signaling pathways during cancer progression. *A,* gene interaction network demonstrating statistical overrepresentation of the EGF signaling pathway. Genes are represented as nodes and the biological relationship between two nodes is represented as an edge (*solid line,* direct association; *dashed line,* indirect association). All edges are supported by at least one reference from the literature, a textbook, or canonical information stored in the Ingenuity Pathways Knowledge Base. *B,* real-time PCR analysis was performed to evaluate the expression levels of Jun and Fos using total RNA from normal prostate, dysplasia/low-grade PIN, high-grade PIN/cancer, or androgen-independent high-grade PIN/cancer (six independent samples per group). Expression levels were standardized *GADPH* (internal control) and plotted using Prism box and whiskers graph. *C,* protein extracts were prepared from mouse tissues from 12-mo wild-type mice (*Nkx3.1*$^{+/+}$*; Pten*$^{+/+}$; normal) or from *Nkx3.1*$^{+/-}$*; Pten*$^{+/-}$ mutant mice with high-grade PIN and cancer, or androgen independent high-grade PIN and cancer or from the indicated mouse or human cell lines. Western blot analyses were performed using the indicated antibodies to detect Fos or Jun, or tubulin as a control for protein loading. *D,* immunohistochemical analyses was performed using the indicated antibodies on sections from the anterior prostate of wild-type mice (*Nkx3.1*$^{+/+}$*; Pten*$^{+/+}$; normal) or from *Nkx3.1*$^{+/-}$*; Pten*$^{+/-}$ mutant mice with high-grade PIN and cancer, or androgen-independent high-grade PIN and cancer. Representative images (*a–f*) are shown from a minimum of eight independent tissues analyzed in each group. *Bars,* 100 μm.

Table 1. Summary of biological pathways and processes significantly overrepresented during cancer progression in the *Nkx3.1; Pten* mutant mice

Gene symbol	Gene name	Affymetrix ID	Fold change	*P*
Category I: genes associated with the EGF signaling pathway				
Egf	*Epidermal growth factor*	1418093_a_at	−4.310	5.62E−02
Fos	*FBJ osteosarcoma oncogene*	1423100_at	2.798	7.06E−02
Grb2	*Growth factor receptor bound protein 2*	1449111_a_at	1.134	3.53E−02
Hras1	*Harvey rat sarcoma virus oncogene 1*	1424132_at	1.049	5.22E−02
Jak1	*Janus kinase 1*	1433804_at	1.594	6.94E−02
Jun	*Jun oncogene*	1448694_at	1.853	4.79E−02
Map3k1	*Mitogen activated protein kinase kinase kinase 1*	1424850_at	2.973	4.97E−03
Mapk3	*Mitogen activated protein kinase 3*	1427060_at	−1.681	2.55E−02
Prkcb1	*Acid phosphatase 1, soluble*	1423478_at	1.085	4.52E−02
		1460419_a_at	1.037	9.51E−02
Srf	*Serum response factor*	1418256_at	−1.212	4.25E−02
Stat1	*Signal transducer and activator of transcription 1*	1450034_at	4.153	5.42E−02
Stat3	*Signal transducer and activator of transcription 3*	1426587_a_at	1.439	1.62E−02
		1460700_at	1.769	3.01E−02
Category II: genes associated with regulation of MAPK activity				
Avpi1	*Arginine vasopressin-induced 1*	1423122_at	1.701	7.27E−02
Cd81	*CD 81 antigen*	1416330_at	2.725	9.63E−05
Cspg4	*Chondroitin sulfate proteoglycan 4*	1450944_at	−1.202	9.49E−02
Dusp16	*Dual specificity phosphatase 16*	1418401_a_at	2.789	1.49E−02
Igh-6	*Immunoglobulin heavy chain 6 (heavy chain of IgM)*	1427329_a_at	−1.047	3.61E−02
		1427351_s_at	1.428	2.55E−02
Map2k3	*Mitogen activated protein kinase kinase 3*	1451714_a_at	−1.477	6.59E−02
Mapk8ip3	*Mitogen-activated protein kinase 8 interacting protein 3*	1425975_a_at	−1.546	2.15E−02
Muc20	*Mucin 20*	1451786_at	2.127	4.13E−02
Plce1	*Phospholipase C, epsilon 1*	1452398_at	1.893	1.49E−02
Ptpn11	*Protein tyrosine phosphatase, non–receptor type 11*	1427699_a_at	−2.404	3.22E−02
		1451225_at	−1.742	1.77E−02
Spred1	*Sprouty protein with EVH-1 domain 1, related sequence*	1423162_s_at	−1.742	6.76E−02
Syk	*Spleen tyrosine kinase*	1418261_at	1.270	9.32E−02
Tirap	*Toll-interleukin 1 receptor domain-containing adaptor protein*	1418685_at	1.391	9.15E−02
Trib3	*Tribbles homologue 3 (Drosophila)*	1426065_a_at	−1.416	4.77E−03
		1456225_x_at	−1.468	5.23E−02
Category III: small GTPase–mediated signal transduction				
5430435G22Rik	*RIKEN cDNA 5430435G22 gene*	1435830_a_at	1.145	6.54E−02
		1424987_at	1.417	9.80E−02
6530401C20Rik	*RIKEN cDNA 6530401C20 gene*	1455008_at	−1.337	5.76E−02
Arf4	*ADP-ribosylation factor 4*	1439367_x_at	−1.063	1.96E−02
Arfip2	*ADP-ribosylation factor interacting protein 2*	1424240_at	−1.232	1.74E−02
Arhgap5	*Rho GTPase activating protein 5*	1450897_at	1.706	3.37E−02
Arl3	*ADP-ribosylation factor-like 3*	1450706_a_at	−2.762	4.94E−02
Arl4	*ADP-ribosylation factor-like 4*	1425411_at	−1.385	6.75E−02
AW742319	*Expressed sequence AW742319*	1433706_a_at	1.740	3.30E−02
		1454698_at	1.600	4.88E−02
B230208H17Rik	*RIKEN cDNA B230208H17 gene*	1435067_at	−1.563	1.97E−03
		1452370_s_at	−1.608	2.98E−02
Baiap2	*Brain-specific angiogenesis inhibitor 1-associated protein 2*	1451027_at	−1.355	9.51E−02
Cdc42	*Cell division cycle 42 homologue (S. cerevisiae)*	1460708_s_at	1.461	8.36E−02
Ctnnal1	*Catenin (cadherin associated protein), α-like 1*	1420930_s_at	−2.506	2.62E−02
Dab1	*RIKEN cDNA C630028C02 gene*	1435578_s_at	−1.333	4.06E−02
Diras1	*DIRAS family, GTP-binding RAS-like 1*	1451820_at	−1.111	6.56E−02
Eral1	*Era (G-protein)-like 1 (E. coli)*	1460548_a_at	−1.153	2.72E−02
		1420520_x_at	−1.138	9.44E−02
Grb2	*Growth factor receptor bound protein 2*	1449111_a_at	1.134	3.53E−02

(*Continued on the following page*)

Table 1. Summary of biological pathways and processes significantly overrepresented during cancer progression in the *Nkx3.1; Pten* mutant mice (Cont'd)

Gene symbol	Gene name	Affymetrix ID	Fold change	*P*
Hras1	*Harvey rat sarcoma virus oncogene 1*	1424132_at	1.049	5.22E−02
Hrasls	*HRAS-like suppressor*	1422919_at	−1.217	8.47E−02
Iqgap1	*IQ motif containing GTPase activating protein 1*	1434998_at	1.519	1.82E−02
		1417379_at	1.967	3.89E−02
LOC544963	*IQ motif containing GTPase activating protein 2*	1459894_at	−2.457	4.06E−02
Ngfa	*Nerve growth factor, α*	1450222_x_at	−1.054	9.46E−02
Notch2	*Notch gene homologue 2 (Drosophila)*	1455556_at	4.084	1.40E−03
Plce1	*Phospholipase C, epsilon 1*	1452398_at	1.893	1.49E−02
Rab10	*RIKEN cDNA 1700012B15 gene*	1429296_at	−1.587	7.09E−02
Rab15	*RAB15, member RAS oncogene family*	1417829_a_at	1.511	8.72E−02
Rab2	*RAB2, member RAS oncogene family*	1419946_s_at	−1.511	4.86E−02
		1449676_at	−1.318	8.30E−02
Rab31	*RIKEN cDNA 1700093E07 gene*	1416165_at	1.462	1.82E−02
Rab32	*RAB32, member RAS oncogene family*	1416527_at	1.585	3.70E−02
Rab33b	*RAB33B, member of RAS oncogene family*	1423083_at	−1.647	2.61E−02
Rab3a	*RAB3A, member RAS oncogene family*	1422589_at	−1.252	1.03E−02
Rab3d	*RAB3D, member RAS oncogene family*	1418891_a_at	−2.646	3.16E−03
		1449259_at	−1.873	1.20E−02
		1418890_a_at	−1.730	5.46E−02
Rab40b	*Rab40b, member RAS oncogene family*	1436566_at	−1.661	1.30E−02
Rab40c	*Rab40c, member RAS oncogene family*	1424331_at	−1.171	9.22E−02
Rab4b	*RAB4B, member RAS oncogene family*	1451643_a_at	1.198	8.06E−03
Rab8a	*RAB8A, member RAS oncogene family*	1418692_at	1.040	3.37E−02
Rab8b	*RAB8B, member RAS oncogene family*	1426799_at	1.017	1.44E−02
Rabl4	*RAB, member of RAS oncogene family-like 4*	1434299_x_at	−1.112	4.80E−03
		1435736_x_at	−1.071	1.04E−02
Ralb	*V-ral simian leukemia viral oncogene homologue B (ras related)*	1417744_a_at	1.341	4.75E−02
Ran	*RAN, member RAS oncogene family*	1438977_x_at	1.946	2.66E−03
		1439270_x_at	1.825	4.24E−03
		1434578_x_at	1.799	1.19E−02
		1433569_x_at	1.844	3.76E−02
Rap1a	*RAS-related protein-1a*	1448020_at	−1.587	4.14E−02
Rap2a	*RAS related protein 2a*	1426965_at	1.679	2.92E−02
Rap2c	*RAP2C, member of RAS oncogene family*	1437016_x_at	1.357	4.80E−02
		1460430_at	1.129	8.33E−02
Rasd1	*RAS, dexamethasone-induced 1*	1423619_at	1.373	5.99E−02
Rasgrf1	*RAS protein-specific guanine nucleotide-releasing factor 1*	1424734_at	−1.189	9.69E−02
Rgl1	*Ral guanine nucleotide dissociation stimulator,-like 1*	1449124_at	−1.259	8.61E−02
Rhoc	*Ras homologue gene family, member C*	1435394_s_at	2.871	2.79E−02
Rhog	*Ras homologue gene family, member G*	1422572_at	1.115	8.07E−02
Rhou	*Ras homologue gene family, member U*	1449028_at	7.100	4.03E−04
		1449027_at	5.127	4.87E−03
Rit1	*Ras-like without CAAX 1*	1428710_at	−1.170	5.14E−02
		1420540_a_at	−1.232	5.29E−02
Rsu1	*Ras suppressor protein 1*	1419259_at	1.198	5.24E−02
Sdcbp	*Syndecan binding protein*	1450941_at	1.822	2.56E−02
Tiam1	*T-cell lymphoma invasion and metastasis 1*	1418057_at	−1.093	3.80E−02
Vav3	*Vav 3 oncogene*	1448600_s_at	1.678	3.16E−04
		1417122_at	1.313	2.74E−02
Category IV: oxygen and reactive oxygen species metabolism				
2600005C20Rik	*RIKEN cDNA 2600005C20 gene*	1452118_at	−1.484	5.62E−02
		1452119_at	−1.026	4.36E−02
Aass	*Aminoadipate-semialdehyde synthase*	1423523_at	−3.106	2.01E−03
Cat	*Catalase*	1416429_a_at	1.859	4.68E−03
Ctsb	*Cathepsin B*	1417490_at	2.956	7.07E−02

(*Continued on the following page*)

Table 1. Summary of biological pathways and processes significantly overrepresented during cancer progression in the *Nkx3.1; Pten* mutant mice (Cont'd)

Gene symbol	Gene name	Affymetrix ID	Fold change	*P*
		1417492_at	2.007	8.93E−02
		1417491_at	1.376	2.74E−02
Cyba	*Cytochrome b-245, α polypeptide*	1454268_a_at	4.175	5.46E−02
Gpx2	*Glutathione peroxidase 2*	1449279_at	4.624	2.42E−02
Gpx3	*Glutathione peroxidase 3*	1449106_at	−5.263	3.70E−02
Gpx4	*Glutathione peroxidase 4*	1456193_x_at	−1.064	4.24E−03
Idh1	*Isocitrate dehydrogenase 1 (NADP+), soluble*	1422433_s_at	3.323	1.77E−02
Ncf2	*Neutrophil cytosolic factor 2*	1448561_at	1.097	7.23E−02
Noxo1	*NADPH oxidase organizer 1*	1425151_a_at	7.005	1.72E−02
Nqo1	*NAD(P)H dehydrogenase, quinone 1*	1423627_at	−1.295	3.70E−02
Prdx1	*Peroxiredoxin 1*	1434731_x_at	1.718	5.55E−03
		1436691_x_at	1.471	1.54E−02
Prdx2	*Peroxiredoxin 2*	1430979_a_at	1.506	8.66E−02
Prdx6	*Peroxiredoxin 6*	1423223_a_at	−2.874	8.11E−03
Txnip	*Thioredoxin interacting protein*	1415996_at	2.453	4.18E−02
Txnrd2	*Thioredoxin reductase 2*	1449097_at	−1.484	2.38E−02

NOTE: Biological pathways and processes statistically overrepresented from probe sets differentially expressed between normal, dysplasia/low-grade PIN, high-grade PIN/cancer, androgen-independent–high-grade PIN, and androgen-independent–cancer–metastases phenotypes. Transcripts were queried for functional enrichment using the Database for Annotation, Visualization and Integrated Discovery 2007. Fold change compares the high-grade PIN–cancer group with normal.

alone (Fig. 3*E, a–h*; Supplementary Fig. S1). Notably, tumors from cells coexpressing Fos and Jun also displayed robust activation of Erk MAPK, evident by Western blot analyses (Fig. 3*A*) and by immunohistochemistry (Fig. 3*E, i–l*).

Interestingly, whereas the Fos- and Jun-expressing cells developed tumors in the intact (noncastrated) hosts, they failed to do so in the castrated hosts (data not shown), consistent with observations of a more stringent requirement for androgen-independent growth *in vivo* than in culture (12). Therefore, Fos and Jun (*a*) display elevated expression in advanced prostate cancer in *Nkx3.1; Pten* mutant mice, where they are correlated with activation of Erk MAPK signaling; and (*b*) function cooperatively to promote prostate tumorigenicity and support androgen-independent growth, although they are not sufficient for androgen independence *in vivo*.

Expression of Fos and Jun in human prostate cancer is associated with cancer progression and activation of Erk MAPK signaling. To examine the expression of Fos and Jun in human prostate cancer, we used two informative sets of human TMAs, which enabled evaluation of their relationship to disease progression (progression TMA) and disease outcome (outcomes TMA; refs. 34, 35). The progression TMA contains 169 informative tissue specimens (each in triplicate), including 35 cases of benign prostate, 27 cases of high-grade PINs, 35 primary tumors (Gleason grade 6–9), and 72 metastatic tumors (34). Interrogation of this TMA revealed that Fos and Jun are preferentially expressed in more advanced disease stages, where they are localized to nuclei of prostate epithelial cells (Fig. 4*A*).

Specifically, Fos and Jun expression (i.e., scoring ≥1.0) was observed in 40% and 34% (14 of 35 and 12 of 35 cases) of localized prostate tumors and 58% (41 of 71 and 42 of 72 cases) of metastatic tumors, respectively, compared with 22% or 11% (6 of 27 or 3 of 27) of PIN lesions and 5% or 0% (2 of 35 or 0 of 35) of benign tissues (Fig. 4*A*). Logistic regression analyses confirmed a significant association of Fos and Jun with advanced disease [Fos: odds ratio (OR), 2.46; 95% confidence interval (95% CI), 1.73-3.51; $P < 0.0001$; Jun: OR, 3.80; 95% CI, 2.37-6.11; $P < 0.0001$].

Furthermore, Jun and Fos were coexpressed in 41 of 55 of the localized or metastatic tumors (Spearman correlation, 0.614; $P < 0.0001$); however, the intensity of Fos staining was typically greater than that of Jun, as we had observed in *Nkx3.1; Pten* mice (see Fig. 2). Notably, their coexpression in human prostate cancer is consistent with our functional analyses showing that Fos and Jun cooperate in prostate tumorigenesis in the *Nkx3.1; Pten* mice (see Fig. 3), as well as their known functions as a heterodimeric transcription factor complex (14).

Based on our gene expression profiling analyses as well as expression and functional validation studies indicating that Fos and Jun may be activated as a consequence of EGF and/or MAPK signaling in *Nkx3.1; Pten* mice (see Figs. 3*A* and 4), we compared the expression of Fos and Jun to that of activated Erk MAPK, which we had previously evaluated using this progression TMA (12). We found that a significant number of the primary and metastatic tumors that expressed activated Erk (i.e., scoring ≥1.0) also expressed Fos and/or Jun (Fig. 4*B* and *C*). In particular, coexpression of activated Erk with Fos and Jun occurred in 14 of 21 cases, with Fos alone in 18 of 21 cases and Jun alone in 16 of 21 cases (Spearman correlation for Fos = 0.398, $P = 0.0009$; Spearman correlation for Jun = 0.298, $P = 0.0152$). These data support our findings from the *Nkx3.1; Pten* mice that these AP-1 transcription factors, and particularly Fos, are downstream effectors of EGF-MAPK signaling in advanced prostate cancer.

Expression of Jun in human prostate cancer is associated with disease outcome. Finally, we investigated the relationship of Fos and Jun expression to clinical outcome using the outcomes TMA set. This comprehensive TMA series contains 948 cases (each in triplicate), of which 842 were informative, all from patients with localized disease (ref. 35; Supplementary Table S3). The primary

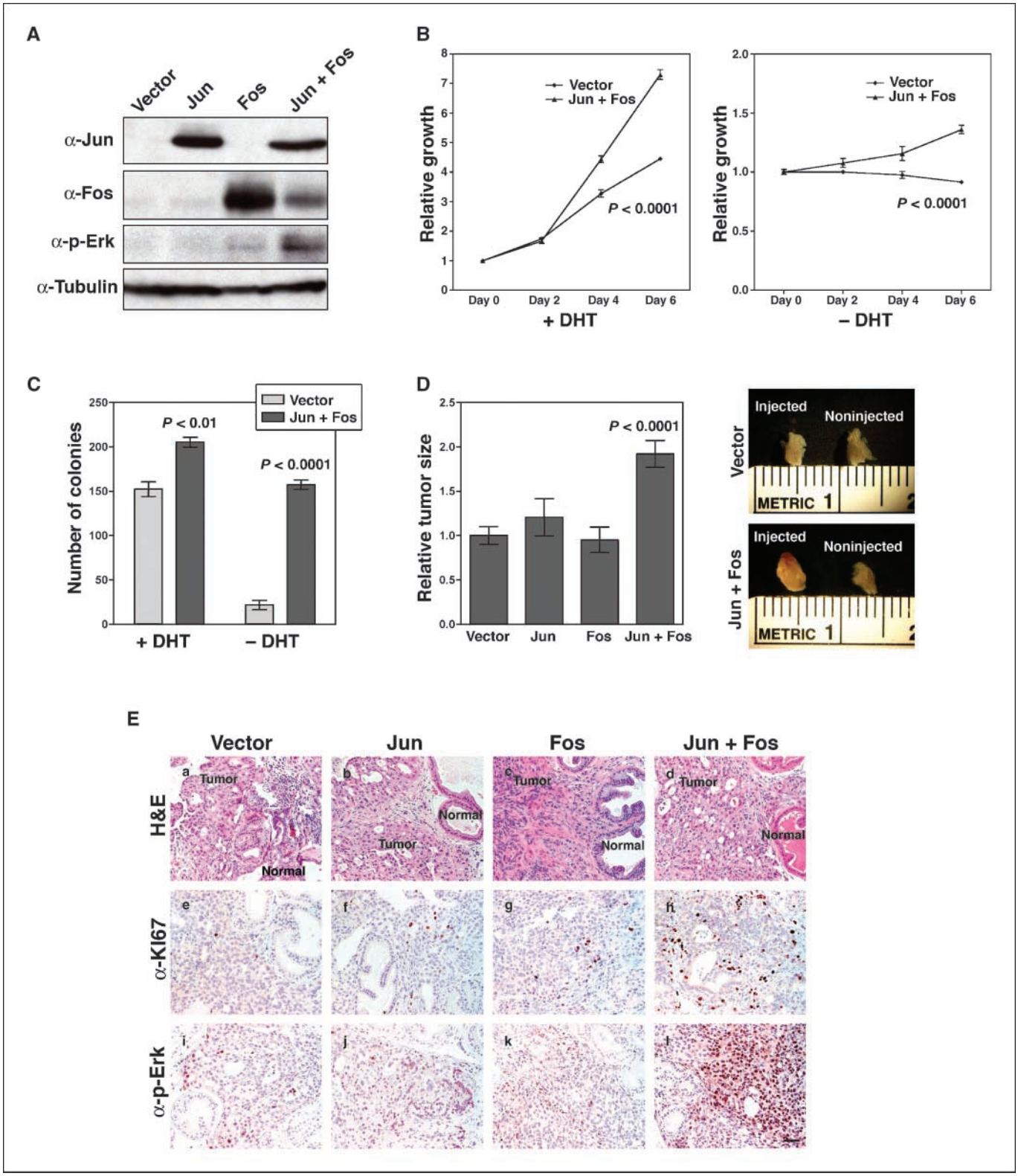

Figure 3. Fos and Jun promote prostate tumorigenicity and activation of Erk MAPK signaling in the *Nkx3.1; Pten* mutant mice. *A,* Western blot analyses were performed using whole-cell protein extracts from CASP 2.1 cells expressing Jun and/or Fos (or a control vector) using the indicated antibodies. Proliferation (*B*) and anchorage-independent (*C*) assays were done using CASP2.1 cells expressing Fos and/or Jun (or a control vector) that had been grown in medium depleted of androgens (*−DHT*) or supplemented with androgens (*+DHT*). Representative assays done in triplicate. *Bars,* SE. Experiments were repeated a minimum of five times with comparable results. *D,* orthotopic tumor assays were performed on CASP 2.1 cells expressing Jun and/or Fos (or a control vector) by unilateral injection into the left dorsal prostate of a *nude* male mouse and grown for 8 wk. *Left,* tumor weights relative to control vector from a minimum of 10 mice per group; *right,* representative images of dorsal prostate lobes showing the injected and noninjected sides. *E,* sections from orthotopic tumors grown in the prostates of the *nude* male mice and analyzed by H&E analyses (*a–d*) or immunostaining for Ki67 (*e–h*) or activated Erk MAPK (*p-Erk, i–l*) as indicated. The normal (host) and tumor regions are indicated. *Bars,* 100 μm.

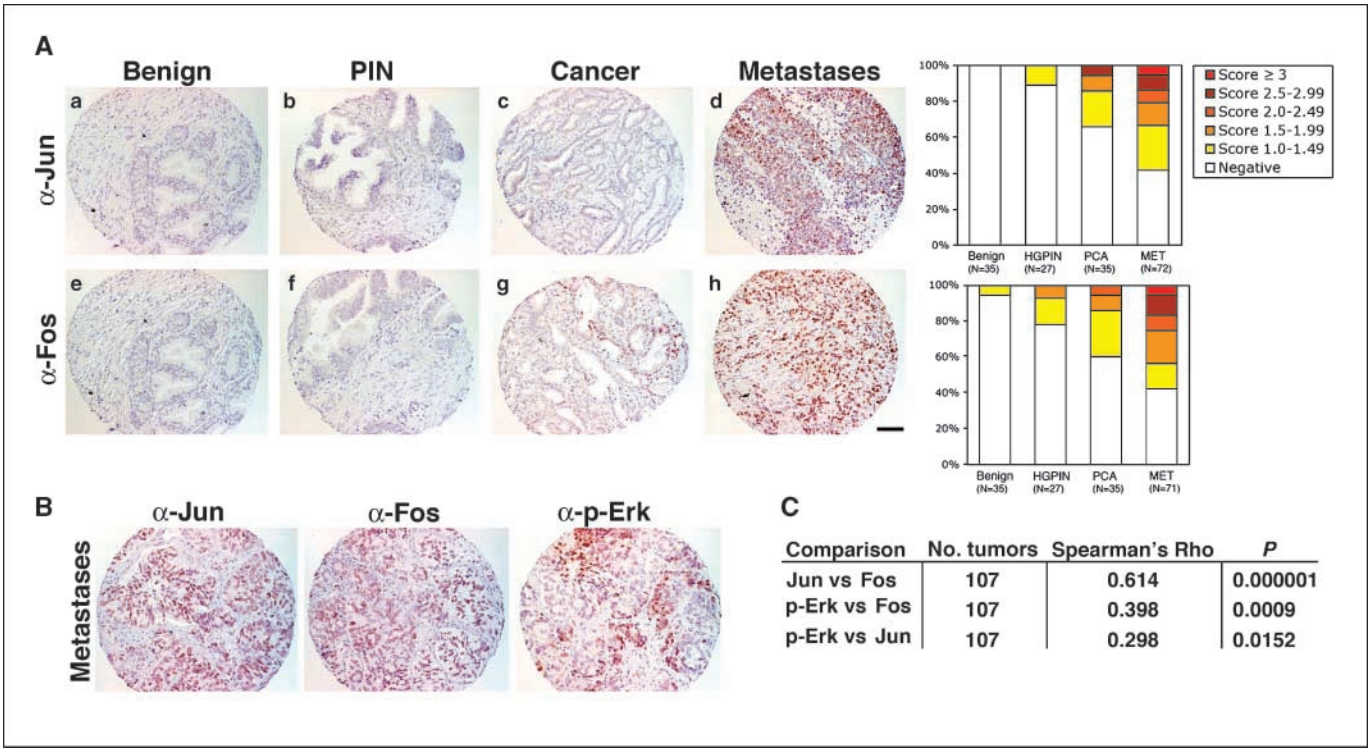

Figure 4. The expression of Fos and Jun in human prostate cancer is associated with cancer progression and activation of Erk MAPK signaling. *A,* expression of Jun and Fos on the progression TMA. Representative images from benign, high-grade PIN, carcinoma, and metastatic specimen immunostained for Jun or Fos, as indicated. *Right,* summary of the percentage of samples stained and relative expression levels. *B,* comparison of expression of activated Erk (*p-Erk*) and Fos and Jun. Representative images illustrate p-Erk, Jun, and Fos expression in a metastatic specimen. *C,* summary of the association of Fos and Jun expression to each other and to p-Erk.

tumors represented on the TMA show a broad spectrum of the disease, corresponding to clinical stages T_1 (50%), T_2 (26%), and T_3 (24%) and pathologic Gleason scores ranging from ≤6 (36%), 7 (54%), and ≥8 (10%). Notably, this TMA includes 201 cases from patients who subsequently experienced biochemical recurrence (stringently defined as a rising PSA of at least 0.2 ng/mL) and 71 cases from patients with clinical failure (defined as clinical evidence of metastases, death from disease, or an increasing PSA in a castrated state). The median follow-up for patients who did not recur was 6.1 years.

The distribution of percentage of positive tumor cells for Jun and Fos expression among these 842 patients is summarized in Supplementary Table S3 and shown in Supplementary Fig. S2. The majority of cases expressed low levels (≤10% positive cells) of Fos and Jun (n = 640 of 824, 76%; and n = 552 of 837, 66%, respectively), whereas a small percentage had higher-level (>50% of positive cells) expression (n = 23 of 824, 3%; and n = 37 of 837, 4%, respectively). Comparison of Fos or Jun expression relative to the pathologic characteristics of the tumor specimens revealed no significant association with pathologic features such as the presence or absence of extracapsular extension, lymph node involvement, and pathologic grade (Gleason ≤6 versus 7 versus ≥8). However, we observed a significant association between expression of Fos (but not Jun) and seminal vesicle invasion (P = 0.016; Supplementary Table S4).

To evaluate the relationship of Fos and Jun expression to disease outcome, we performed univariate analysis (Fig. 5). Although there was no apparent association between the percentage of Fos-expressing cells and biochemical recurrence [hazard ratio (HR), 1.01 for each 5% increase; 95% CI, 0.97, 1.06; P = 0.6], higher levels of Jun-positive tumor cells increased the risk of biochemical recurrence (HR, 1.04 for each 5% increase; 95% CI, 1.00, 1.08; P = 0.054). This relationship of Jun, but not Fos, expression to biochemical recurrence is further illustrated in the Kaplan-Meier plot, showing that patients with high levels of Jun expression (>50% positive cells) had a higher probability of recurrence than patients with lower levels of expression (<50% positive cells; P = 0.003; Fig. 5). In contrast, patients with low (<50% positive cells) and high (>50% positive cells) levels of Fos expression had a similar probability of recurrence (P = 0.9; Supplementary Fig. S3). Interestingly, in contrast to biochemical recurrence, we observed no significant association between Jun expression and clinical failure (HR, 1.00 for each 5% increase; 95% CI, 0.93-1.07; P = 0.9). Taking into consideration that the expression of Fos and Jun was skewed such that majority of the tumors had a low percentage of expression (Supplementary Fig. S2), we verified these results using log-transformed values, which further confirmed our finding that expression of Jun is associated with biochemical recurrence.

We further examined the positive association of Jun expression with biochemical recurrence using multivariable analysis. After adjusting for PSA and pathologic stage and grade, the percentage of Jun-positive tumor cells continued to show an association with outcome (HR, 1.04 for each 5% increase; 95% CI, 1.00-1.08; P = 0.050) although it did not importantly improve the predictive accuracy of a model including PSA, pathologic stage, and grade (c-index = 0.784 and 0.787, respectively, for model without and with Jun). In summary, these data indicate that the expression of Jun is associated with relapse-free survival in men with prostate cancer

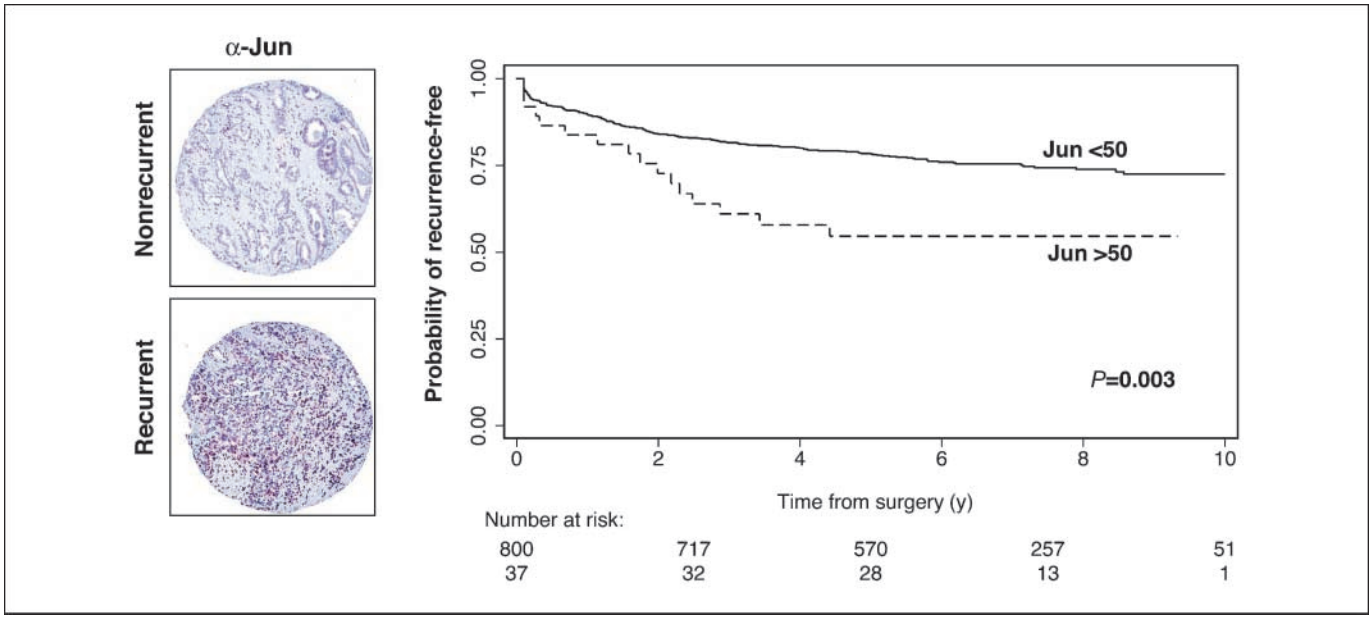

Figure 5. Expression of Jun in human prostate cancer is associated with disease outcome. Expression of Jun on the outcomes TMA. *Left,* representative images of tumors stained for Jun from patients that did not display biochemical recurrence within the 6.1-y follow-up period (*Nonrecurrent*) or those that displayed biochemical recurrence (*Recurrent*). *Right*, Kaplan-Meier probability of freedom of biochemical recurrence relative to expression levels.

and suggest that this association is largely independent of previously described prognostic indicators.

Conclusions

There is now mounting evidence demonstrating the value of interrogating mouse models of cancer to gain molecular insights into the mechanisms of human cancer. Nonetheless, there are still relatively few examples in which insights from mouse studies have provided insights that may directly affect the prognosis or treatment of cancer patients. Here, we have shown that the analyses of mouse models has led to the identification of Jun as a bona fide marker of aggressive prostate cancer, which is associated with disease recurrence (Fig. 6).

Originally identified as viral oncogenes, several studies have shown an association between c-*Fos* and/or c-*Jun* expression and

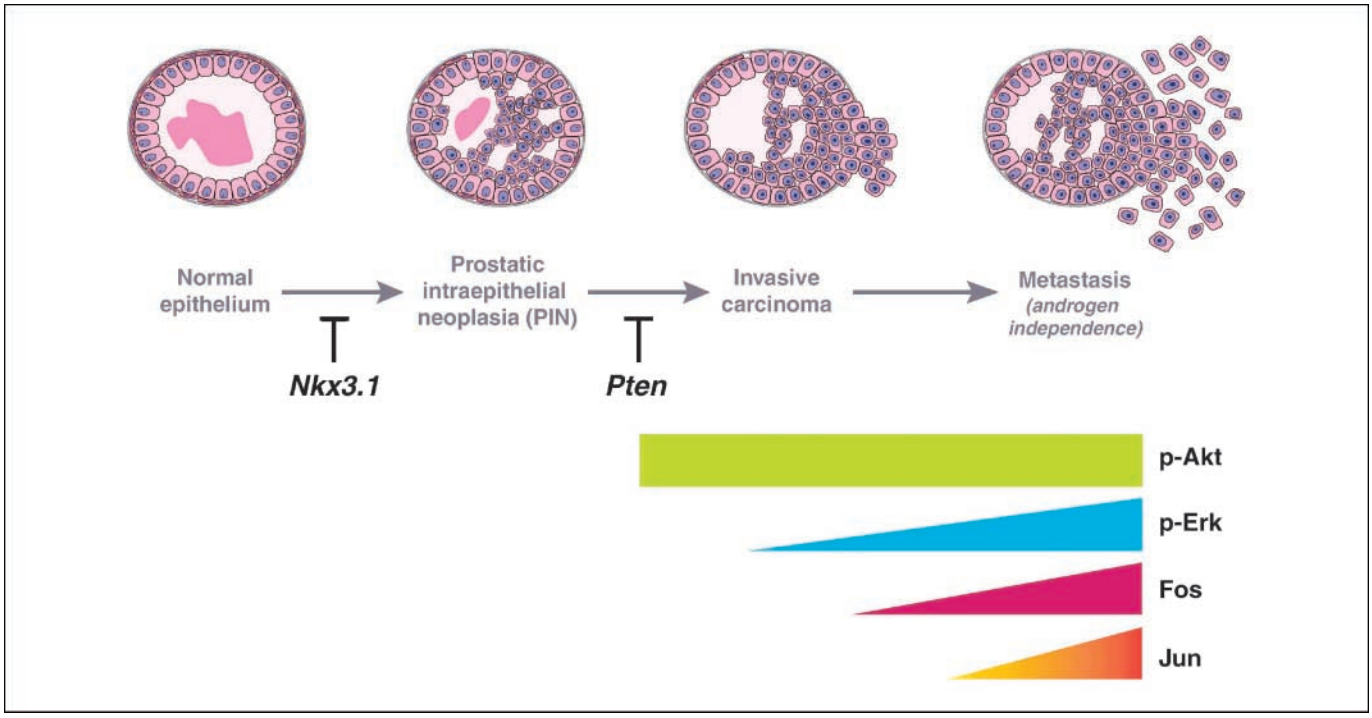

Figure 6. A model depicting the relationship of Fos, Jun, and selected kinase signaling pathways to cancer progression in the context of loss of function of *Nkx3.1* and *Pten*, as further discussed in the text.

the degree of malignancy and/or invasive potential in cancers of the bone, skin, breast, and immune system (27, 36–41). Furthermore, disruption of *Fos* or *Jun* function in mutant mice directly contributes to the development of tumors of the muscle, skin, and bone (38, 42, 43). However, few studies have shown a direct causal role for Fos or Jun in human cancer (e.g., refs. 44, 45). Our integrated functional studies in mutant mice and informed expression analyses of human prostate cancer indicate a causal role for Fos and Jun in prostate cancer malignancy. Notably, the relevance of Jun for prostate cancer is further supported by a recent study showing that c-Jun-NH_2-kinase kinase, which phosphorylates and activates c-Jun, is up-regulated in human prostate cancer (46). Considering the link between Fos and Jun expression and activation of the EGF and MAPK signaling pathways, we suggest that Fos and Jun are potential targets for therapeutic intervention, particularly in patients that display activated Erk MAPK signaling.

Although their deregulated expression is widely associated with many types of cancers, Fos and Jun may have a unique role in prostate tumorigenesis because of their relevance for androgen receptor signaling. As is the case for other nuclear hormone receptors, Fos and Jun regulate the transcriptional activity of the androgen receptor (30, 31, 47), which may provide a mechanism by which they promote prostate tumorigenesis. Notably, previous studies have shown that Fos and Jun protein expression is up-regulated in hormone-refractory prostate cancer (28, 29). Although the TMAs used in the current study do not directly address the relationship of Fos and Jun expression to androgen independence, most of the metastases in the progression TMA were from hormone-refractory patients (34); moreover, we also found that Fos and Jun were clearly elevated in androgen-independent tumors in our mouse model. Interestingly, it has been suggested that the activities of Fos and Jun in breast cancer may be attributed to their actions on estrogen receptor, another member of the nuclear hormone receptor family (48).

Finally, although our findings suggest that Fos and Jun function cooperatively in prostate tumorigenesis, their relative contributions do not seem to be equivalent, because the expression of Jun, but not that of Fos, is associated with disease recurrence. Indeed, Fos and Jun are coexpressed in many primary and metastatic tumors, but Fos is consistently expressed at higher levels and is more significantly associated with activation of Erk MAPK signaling. This may reflect the ability of Fos to form heterodimeric complexes with other Jun-related proteins as well as members of the Atf transcription factor family, which might result in distinct transcriptional activities from those of Fos-Jun heterodimers (36). In particular, we have observed that several other members of the Jun and Atf families are deregulated during cancer progression in *Nkx3.1; Pten* mice (Supplementary Data), and are expressed in human prostate cancer as well (49). Therefore, we propose that Fos, which is broadly expressed in prostate cancer, forms heterodimeric complexes with multiple Jun and Atf family proteins, whereas expression of Jun and formation of Fos-Jun heterodimers is more restricted to subsets of tumors (Fig. 6).

According to this model (Fig. 6), expression of Jun would serve a pivotal role in malignant progression, which is consistent with its association with disease recurrence as well as the observed cooperativity of Fos and Jun in prostate tumorigenicity. Thus, analyses of Jun may provide insights into the molecular pathways that lead to aggressive forms of prostate cancer, as well as serve as a target for therapeutic intervention.

Acknowledgments

Received 10/31/2007; accepted 1/15/2008.

Grant support: UO1CA84294 and CA115717 (C. Abate-Shen), CA115985 (M.M. Shen), CA-72720-10 (W-J. Shih and Y. Lin) P50CA092629 (P.T. Scardino, W.L. Gerald, A.J. Vickers, V.E. Reuter, and A.M. Serio), and T32 HL07382-30 (WJ. Jessen). Preparation of the TMAs was supported by grants U01-CA084999 (W.L. Gerald) and P50CA092629 (P.T. Scardino).

The costs of publication of this article were defrayed in part by the payment of page charges. This article must therefore be hereby marked *advertisement* in accordance with 18 U.S.C. Section 1734 solely to indicate this fact.

References

1. DeMarzo AM, Nelson WG, Isaacs WB, Epstein JI. Pathological and molecular aspects of prostate cancer. Lancet 2003;361:955–64.
2. Lin DW, Coleman IM, Hawley S, et al. Influence of surgical manipulation on prostate gene expression: implications for molecular correlates of treatment effects and disease prognosis. J Clin Oncol 2006;24:3763–70.
3. Tinker AV, Boussioutas A, Bowtell DD. The challenges of gene expression microarrays for the study of human cancer. Cancer Cell 2006;9:333–9.
4. Sweet-Cordero A, Mukherjee S, Subramanian A, et al. An oncogenic KRAS2 expression signature identified by cross-species gene-expression analysis. Nat Genet 2005; 37:48–55.
5. Moody SE, Perez D, Pan TC, et al. The transcriptional repressor Snail promotes mammary tumor recurrence. Cancer Cell 2005;8:197–209.
6. Herschkowitz JI, Simin K, Weigman VJ, et al. Identification of conserved gene expression features between murine mammary carcinoma models and human breast tumors. Genome Biol 2007;8:R76.
7. Mulholland DJ, Dedhar S, Wu H, Nelson CC. PTEN and GSK3β: key regulators of progression to androgen-independent prostate cancer. Oncogene 2006;25:329–37.
8. Paez J, Sellers WR. PI3K/PTEN/AKT pathway. A critical mediator of oncogenic signaling. Cancer Treat Res 2003;115:145–67.
9. Shen MM, Abate-Shen C. Roles of the Nkx3.1 homeobox gene in prostate organogenesis and carcinogenesis. Dev Dyn 2003;228:767–78.
10. Shen MM, Abate-Shen C. Pten inactivation and the emergence of androgen-independent prostate cancer. Cancer Res 2007;67:6535–8.
11. Abate-Shen C, Banach-Petrosky WA, Sun X, et al. Nkx3.1; Pten mutant mice develop invasive prostate adenocarcinoma and lymph node metastases. Cancer Res 2003;63:3886–90.
12. Gao H, Ouyang X, Banach-Petrosky WA, Gerald WL, Shen MM, Abate-Shen C. Combinatorial activities of Akt and B-Raf/Erk signaling in a mouse model of androgen-independent prostate cancer. Proc Natl Acad Sci U S A 2006;103:14477–82.
13. Kim MJ, Cardiff RD, Desai N, et al. Cooperativity of Nkx3.1 and Pten loss of function in a mouse model of prostate carcinogenesis. Proc Natl Acad Sci U S A 2002; 99:2884–9.
14. Abate C, Curran T. Encounters with Fos and Jun on the road to AP-1. Semin Cancer Biol 1990;1:19–26.
15. Bhatia-Gaur R, Donjacour AA, Sciavolino PJ, et al. Roles for Nkx3.1 in prostate development and cancer. Genes Dev 1999;13:966–77.
16. Kim MJ, Bhatia-Gaur R, Banach-Petrosky WA, et al. Nkx3.1 mutant mice recapitulate early stages of prostate carcinogenesis. Cancer Res 2002;62:2999–3004.
17. Huang DW, Sherman BT, Tan Q, et al. DAVID Bioinformatics Resources: expanded annotation database and novel algorithms to better extract biology from large gene lists. Nucleic Acids Res 2007;35:W169–75.
18. Harrell F. Regression modeling strategies: with applications to linear models, logistic regression, and survival analysis. New York: Springer; 2001.
19. Chen CD, Welsbie DS, Tran C, et al. Molecular determinants of resistance to antiandrogen therapy. Nat Med 2004;10:33–9.
20. Steinberg J, Oyasu R, Lang S, et al. Intracellular levels of SGP-2 (Clusterin) correlate with tumor grade in prostate cancer. Clin Cancer Res 1997;3:1707–11.
21. Varambally S, Dhanasekaran SM, Zhou M, et al. The polycomb group protein EZH2 is involved in progression of prostate cancer. Nature 2002;419: 624–9.
22. Magee JA, Araki T, Patil S, et al. Expression profiling reveals hepsin overexpression in prostate cancer. Cancer Res 2001;61:5692–6.
23. Weber MJ, Gioeli D. Ras signaling in prostate cancer progression. J Cell Biochem 2004;91:13–25.
24. Eferl R, Wagner EF. AP-1: a double-edged sword in tumorigenesis. Nat Rev Cancer 2003;3:859–68.
25. Vogt PK. Jun, the oncoprotein. Oncogene 2001;20: 2365–77.
26. Ordway JM, Williams K, Curran T. Transcription repression in oncogenic transformation: common targets of epigenetic repression in cells transformed by Fos, Ras or Dnmt1. Oncogene 2004;23:3737–48.
27. Ozanne BW, Spence HJ, McGarry LC, Hennigan RF.

Transcription factors control invasion: AP-1 the first among equals. Oncogene 2007;26:1–10.
28. Edwards J, Krishna NS, Mukherjee R, Bartlett JM. The role of c-Jun and c-Fos expression in androgen-independent prostate cancer. J Pathol 2004;204:153–8.
29. Church DR, Lee E, Thompson TA, et al. Induction of AP-1 activity by androgen activation of the androgen receptor in LNCaP human prostate carcinoma cells. Prostate 2005;63:155–68.
30. Chen SY, Cai C, Fisher CJ, et al. c-Jun enhancement of androgen receptor transactivation is associated with prostate cancer cell proliferation. Oncogene 2006;25:7212–23.
31. Tillman K, Oberfield JL, Shen XQ, Bubulya A, Shemshedini L. c-Fos dimerization with c-Jun represses c-Jun enhancement of androgen receptor transactivation. Endocrine 1998;9:193–200.
32. Sato N, Sadar MD, Bruchovsky N, et al. Androgenic induction of prostate-specific antigen gene is repressed by protein-protein interaction between the androgen receptor and AP-1/c-Jun in the human prostate cancer cell line LNCaP. J Biol Chem 1997;272:17485–94.
33. Chandran UR, Ma C, Dhir R, et al. Gene expression profiles of prostate cancer reveal involvement of multiple molecular pathways in the metastatic process. BMC Cancer 2007;7:64.
34. Holzbeierlein J, Lal P, LaTulippe E, et al. Gene expression analysis of human prostate carcinoma during hormonal therapy identifies androgen-responsive genes and mechanisms of therapy resistance. Am J Pathol 2004;164:217–27.
35. Bjartell A, Al-Ahmadie AA, Serio AM, et al. Association of cysteine-rich secretory protein 3 and b-microseminoprotein with outcome after radical prostatectomy. Clin Cancer Res 2007;13:4130–8.
36. Angel P, Szabowski A, Schorpp-Kistner M. Function and regulation of AP-1 subunits in skin physiology and pathology. Oncogene 2001;20:2413–23.
37. Drakos E, Leventaki V, Schlette EJ, et al. c-Jun expression and activation are restricted to CD30$^+$ lymphoproliferative disorders. Am J Surg Pathol 2007;31:447–53.
38. Fleischmann A, Jochum W, Eferl R, Witowsky J, Wagner EF. Rhabdomyosarcoma development in mice lacking Trp53 and Fos: tumor suppression by the Fos protooncogene. Cancer Cell 2003;4:477–82.
39. Ludes-Meyers JH, Liu Y, Munoz-Medellin D, Hilsenbeck SG, Brown PH. AP-1 blockade inhibits the growth of normal and malignant breast cells. Oncogene 2001;20:2771–80.
40. Milde-Langosch K. The Fos family of transcription factors and their role in tumourigenesis. Eur J Cancer 2005;41:2449–61.
41. Wagner EF, Eferl R. Fos/AP-1 proteins in bone and the immune system. Immunol Rev 2005;208:126–40.
42. Johnson R, Spiegelman B, Hanahan D, Wisdom R. Cellular transformation and malignancy induced by ras require c-jun. Mol Cell Biol 1996;16:4504–11.
43. Zenz R, Scheuch H, Martin P, et al. c-Jun regulates eyelid closure and skin tumor development through EGFR signaling. Dev Cell 2003;4:879–89.
44. Mariani O, Brennetot C, Coindre JM, et al. JUN oncogene amplification and overexpression block adipocytic differentiation in highly aggressive sarcomas. Cancer Cell 2007;11:361–74.
45. Steidl U, Rosenbauer F, Verhaak RG, et al. Essential role of Jun family transcription factors in PU.1 knockdown-induced leukemic stem cells. Nat Genet 2006;38:1269–77.
46. Vivanco I, Palaskas N, Tran C, et al. Identification of the JNK signaling pathway as a functional target of the tumor suppressor PTEN. Cancer Cell 2007;11:555–69.
47. Bubulya A, Wise SC, Shen XQ, Burmeister LA, Shemshedini L. c-Jun can mediate androgen receptor-induced transactivation. J Biol Chem 1996;271:24583–9.
48. DeNardo DG, Kim HT, Hilsenbeck S, Cuba V, Tsimelzon A, Brown PH. Global gene expression analysis of estrogen receptor transcription factor cross talk in breast cancer: identification of estrogen-induced/activator protein-1-dependent genes. Mol Endocrinol 2005;19:362–78.
49. Bandyopadhyay S, Wang Y, Zhan R, et al. The tumor metastasis suppressor gene Drg-1 down-regulates the expression of activating transcription factor 3 in prostate cancer. Cancer Res 2006;66:11983–90.